Supplementary Online Content

Gonzalez-Cao M, Morán T, Dalmau J, et al. Assessment of the feasibility and safety of durvalumab for treatment of solid tumors in patients with HIV-1 infection: the phase 2 DURVAST study. *JAMA Oncol*. Published online April 9, 2020. doi:10.1001/jamaoncol.2020.0465

This supplementary material has been provided by the authors to give readers additional information about their work.

eMETHODS

STUDY DESIGN AND PATIENTS

This is a multicenter, non-randomized, open-label phase 2 trial in HIV-1-infected patients with advanced cancer. The study was conducted in eight hospitals in Spain from Spanish Lung Cancer Group (SLCG). Safety was assessed in all patients. Eligible patients comprised any solid tumor type in which anti-PD-1 or anti-PD-L1 antibodies have previously demonstrated antitumoral activity and undetectable viral load in their last blood analysis. Adverse events were classified as drug-related or unrelated, according to investigator criteria, and were graded with the use of the National Cancer Institute Common Terminology Criteria for Adverse Events (NCI CTCAE), version 4.03. Secondary endpoints of the DURVAST study included objective response rate, duration of response, progression-free survival and overall survival. Tumor measurements were performed every 8 weeks and response was evaluated using Response Evaluation Criteria in Solid Tumors version 1.1 (RECIST 1.1). An exploratory objective of the study was to assess the correlation of the tumor baseline genomic and immune activation status with treatment outcome.

The study was conducted in accordance with the declaration of Helsinki and international conference on harmonization guidelines for good clinical practice.

STATISTICAL ANALYSIS

Disease control rate (DCR) was calculated as the combined rates of complete response, partial response and durable stable disease (≥ 24 weeks). Duration of response was defined as the time between the first objective response and disease progression. The median duration of response and its confidence interval was estimated with the use of Kaplan-Meier method. For progression-free and overall survival, median values and two-sided 95% confidence intervals (95% CI) were estimated with the use of Kaplan-Meier methods. Cox proportional-hazards hazard regression model was applied with potential risk factors as covariates, to estimate Hazard Ratios (HR) and their 95% CI. Summary statistics, frequency tables, and parametric and nonparametric statistical tests were used, as applicable. All P values and confidence intervals were two-sided. Statistical analyses were performed with the use of SAS Software V9.4. Safety and efficacy data are reported as of December 21, 2018.

TUMOR TISSUE AND BLOOD SAMPLES

All patients underwent baseline tumor formalin fixed paraffin-embedded (FFPE) tissue acquisition prior to enrollment. If it was not possible to perform a new biopsy, patients were included if they had an archival tissue biopsy available. PD-L1 immunostaining was performed on tissue biopsies using the commercially available PD-L1 immunohistochemistry 22C3 pharmDxassay (Dako North America). A PD-L1

expression (tumor proportion score [TPS]) level of ≥1% was defined as positive staining. Peripheral blood samples were collected at the following time points: pre-treatment and after 2, 4, 12 and 24 weeks. Patients who continued treatment after 24 weeks provided peripheral blood samples every 12 weeks until disease progression or at least until week 72 in the absence of progression.

RNA isolation and transcriptional analysis

FFPE slides (5 μM) of pre-treatment tumor biopsies from 14 patients were obtained after appropriate written informed consent and stained with hematoxylin and eosin. Tumor area was evaluated by a pathologist, and samples were macro-dissected prior to RNA isolation. Typically, RNA was isolated from 2-4 slides per patient. Total RNA was extracted with the High Pure FFPE RNA Micro Kit (Roche, Indianapolis, IN), following the manufacturer's protocols, and eluted in a final volume of 25 μL. RNA integrity and concentration were evaluated using the 2100 Bioanalyzer (Agilent Technologies) and the RNA 6000 Pico kit (Agilent Technologies). Gene expression analysis was performed on the Nanostring nCounter gene expression platform (NanoString Technologies Inc., Seattle, WA, USA). The Human PanCancer IO 360 code set consisting of a 770-gene panel related to the tumor, microenvironment and immune response was used. Per sample, 10-300 ng of total RNA in a final volume of 5 μL was mixed with 5' reporter probes, tagged with a fluorescent barcode from the codeset, and 3' biotinylated capture probes. Hereafter, probes and target transcripts were hybridized overnight at 65°C for 18 hours, per manufacturer's recommendation. Excess capture and reporter probes were then removed from the reaction mixes using the high sensitivity program of the Nanostring nCounter preparation station. Codeset-RNA complexes were immobilized on a streptavidin-coated cartridge for data collection. Fluorescent barcodes on the surface of the cartridge were counted in the nCounter Digital Analyzer at maximum scan resolution (555 FOVs).

Data normalization and differential expression analysis

Raw reporter counts were preprocessed using the nSolver Analysis Software version 4.0 (NanoString Technologies Inc., Seattle, WA, USA). An initial quality control step was performed for each sample, and counts were then normalized for technical assay variation, using the geometric mean of the positive control targets. Lane-specific gene counts were then multiplied by the obtained normalization factor. Data were normalized for sample input variability using the geometric mean of the most stable set of housekeeping genes and lane-specific normalization factors were calculated. A second quality control step was implemented, where samples with a positive-normalization or content-normalization factor outside of the predefined minimum and maximum threshold (0.3-3.0 and 0.1-10.0, respectively), were excluded from analysis. Data analysis was performed on $\log_2$-transformed data with the nCounter Advanced Analysis Software version 2.0 (NanoString Technologies Inc., Seattle, WA, USA) and R and R-studio version 3.5.3. Fold change in expression of each gene between the two groups was calculated based on the average gene expression of each group. Appropriate statistical testing was performed within the software to determine differentially expressed genes (DEGs) between groups, and nominal p-values and false discovery rate (FDR) adjusted p-values, have been reported. Fold changes and p-values were depicted in volcano plots for visualization, where a fold change of 2 and nominal p-value of <0.05 was used to define DEGs. For the pathway signatures average expression of all genes in one pathway were used to calculate a pathway

score. Differences in pathway signature scores were then determined using a Mann-Whitney U test.

DNA isolation

Purification of cfDNA was performed from 4 mL of plasma using a custom protocol with the QIAsymphony® DSP Virus/Pathogen Midi Kit using a QIAsymphony robot (QIAGEN, Hilden, Germany) and following the manufacturer's instructions. The final elution volume was 50 µL per sample. For liquid biopsies with less than 4 mL, an alternative custom protocol using 1.2 mL and a final elution volume was 30 µL was used. For DNA purification from FFPE samples, the GeneRead DNA FFPE Kit (QIAGEN, Hilden, Germany) was employed, following the manufacturer's instructions. DNA concentration was measured by Qubit®. Samples with ≥2.5 ng DNA/mL were diluted to achieve this concentration.

NGS for mutation testing

Next generation sequencing (NGS) of DNA isolated from either tissue or plasma was performed with the GeneReader Platform (QIAGEN, Hilden, Germany).

Purified DNA (16.5 µL, ~40 ng) was used as a template to generate libraries for sequencing with the GeneReadQIAact Custom DNA Panel, according to manufacturer's instructions. The panel is designed to enrich specific target regions in 20 selected genes frequently altered in solid cancer tumors (*ALK, BRAF, CDK4, CDK6, EGFR, ERBB2, ERBB4, FGFR1, IDH1, IDH2, KIT, KRAS, MET, NRAS, PDGFRA, PIK3CA, RICTOR, ROS1, STK11, TP53*), including *MET* exon 14 skipping mutations. Libraries were quantified using a QIAxcel® Advanced System, diluted to 100 pg/ul and pooled in batches of 6 (liquid biopsies) or 12 (tissues). Clonal amplification was performed on 625 pg of pooled libraries by the GeneRead Clonal Amp Q Kit using the GeneReadQIAcube and an automated protocol. Following bead enrichment, pooled libraries were sequenced using the GeneRead UMI Advanced Sequencing Q kit in a GeneReader instrument. QIAGEN Clinical Insight Analyze (QCI-A) software was employed to perform the secondary analysis of FASTQ reads, align the read data to the hg19 reference genome sequence, call sequence variants and generate a report for visualization of the sequencing results. Variants were imported into the QIAGEN Clinical Insight Interpret (QCI-I) web interface for data interpretation and generation of final custom report.

eRESULTS

RESPONSE

Four patients had partial response (PR), all of them had NSCLC. Among the five patients with stable disease (SD), three had NSCLC, one melanoma and one anal carcinoma. Seven patients (44%) had disease progression (PD) as their best response (**eFig. 2 in the Supplementary Appendix)**.

SURVIVAL ANALYSIS

Median progression-free and overall survival were 2.4 months (95% CI, 1.4-5.3) and 9.2 months (95% CI, 2.3-NR), respectively (**eFig. 3A and 3B in the Supplementary Appendix**).

EARLY DEATHS

There were four early deaths after the first dose of durvalumab. They include two cases with the suspect of death due to rapid tumor progression and two other NSCLC patients that death occurred in the context of tumor progression due to pneumonia and delirium, respectively. Although, per investigator assessment, these adverse events were not drug-related, this cannot be completely excluded.

SUBGROUP ANALYSIS BASED ON PREDICTIVE BIOMARKERS AND ANTIVIRAL THERAPY

Tumor tissue for PD-L1 assessment was available for 15 HIV-1-infected patients in the DURVAST study (**Table 1**) and 13 of them were evaluable for response (**eTable 1**). Among them, PD-L1 was positive for four NSCLC patients, while it was negative for the remaining 11 patients. Objective responses (PRs) were seen in three PD-L1-positive patients (3/4) and in none of the PD-L1-negative patients (0/11), although one patient with PD-L1 negative tumor had a durable stable disease **(eTable 2 in the Supplementary Appendix**). Median progression-free survival was 5.3 months (95% CI, 3.4-NR) for PD-L1 positive patients versus 1.8 months (95% CI, 1.2-6) for the PD-L1 negative patients (P=0.3467) (**eFig. 4A in the Supplementary Appendix**). Median overall survival was NR for PD-L1 positive patients versus 6.9 months (95% CI, 1.2-13) for the PD-L1 negative patients (P=0.0644) (**eFig. 4B in the Supplementary Appendix**).

Molecular classification of either tumor tissue or circulating-free DNA (cfDNA) was performed in 18 patients. *KRAS* mutations were detected in six, *TP53* mutations in eight, and *STK11* mutations in three HIV-1-infected NSCLC patients (**eTable 3 in the Supplementary Appendix**). No correlation was found between the presence of the gene mutations and treatment outcome.

To explore if gene expression analysis of pre-treatment tumor tissue can predict which patients will derive clinical benefit (defined as PR or SD for at least 24 weeks) from durvalumab treatment, an analysis was performed on baseline tumor tissue samples of 14 HIV-positive cancer patients, enrolled in the DURVAST trial. The nCounter PanCancer IO 360 panel (NanoString Technologies Inc., Seattle, WA, USA) was used for this purpose and contains 770 genes involved in tumor biology, microenvironment and immune response. Pre-treatment gene expression profiles (GEPs) were correlated with clinical benefit to durvalumab treatment, and an initial exploratory analysis revealed differentially expressed genes (DEGs) between the patients with and without clinical benefit. Expression of a combined biological signature, including cytokine and chemokine signaling nodes and transforming growth factor-beta (TGF-beta) signaling pathway components, yielded significantly different results between patients with and without clinical benefit (defined as PR or SD for at least 24 weeks) (P = 0.017) (**eFig. 5 and 6 and eTable 4 in the Supplementary Appendix**).

Further exploration, using panel-incorporated biological signatures related to tumor and immune activities, were evaluated and some of the most DEGs (based on higher log2 fold change values and P <0.05) were shown to be involved in cytokine and chemokine signaling. Although not significant, patients without clinical benefit tend to have lower expression of genes involved in cytokine and chemokine signaling (P = 0.097) (**eFig. 6A in the Supplementary Appendix**), amongst which CCL3 (log2 fold change = -5.32; P < 0.05) and CCL4 (log2 fold change = -4.19; P <0.05). The chemokines CCL3 and CCL4 were previously shown to have a critical role in immune-cell recruitment to the tumor site and to induce an antigen-specific T cell response by regulating lymph node homing[1]. Moreover, blocking CCL3 and CCL4 reduced the production of antigen-specific CD8+ T cells, decreasing their ability to effectively kill malignant cells[2]. Since cytokines and chemokines are important for regulating immune and inflammatory responses by activating the innate and adaptive immune system, insufficient pre-treatment production may predict worse response to immunotherapy.

In contrast, other DEGs were involved in the biological signature of TGF beta, pointing towards immunosuppressive mechanisms like drug resistance and induction of epithelial to mesenchymal transition[3]. TGF beta can shape the tumor microenvironment, and prevent entry of CD8+ T cells[4]. In addition, TGF beta was shown to drive immune evasion, while its inhibition reduced tumor burden and metastasis[5]. In the current exploratory analysis, patients without clinical benefit to durvalumab tend to have a higher TGF beta signature score compared to patients with clinical benefit (P= 0.318) (**eFig. 6B in the Supplementary Appendix**). The most DEG contained in this signature is CDKN2B (log2 fold change = 2.28; P<0.05), and its expression was previously found to be induced by TGF beta[6].

Baseline activation of the immune system in the tumor microenvironment, combined with related immunosuppressive signals may have a better predictive value than each expression signature by itself. When combining both signatures for all patients, we obtained an aggregated differential expression value that was significantly different between the patients with and without clinical benefit (P= 0.017) (**eFig. 6C in the Supplementary Appendix**).

Finally, we opted to see whether cART with either INSTIs or non-INSTIs had an impact on the treatment outcome of the HIV-1-infected cancer patients in the DURVAST study. As shown in **eTable 1**, HIV-1-infected cancer patients on cART with NRTIs + INSTIs had a significantly longer duration of clinical benefit with durvalumab, compared to those on cART with NRTIs + non-INSTIs (P=0.0364).

SUPPLEMENTARY TABLES

eTable 1. Drug related adverse events (AEs).

Type of adverse events– n (%)	Grade 1	Grade 2	Grade 3-5
Any	7 (35)	3 (50)	0 (0)
Respiratory infection	0 (0)	0 (0)	0 (0)
Neurological disorders	0 (0)	0 (0)	0 (0)
Hypotension	0 (0)	0 (0)	0 (0)
Fever	0 (0)	0 (0)	0 (0)
Arthromyalgia	4 (20)	1 (5)	0 (0)
Asthenia	3 (15)	1 (5)	0 (0)
Nausea-vomiting	2 (10)	0 (0)	0 (0)
Diarrhea	2 (10)	1 (5)	0 (0)
Skin AEs	3 (15)	0 (0)	0 (0)
Neutropenia	0 (0)	1 (5)	0 (0)

eTable 2. Outcome to durvalumab based on the type of cART.

cART	N	Response	Duration of clinical benefit		Progression-free survival		Overall survival	
			Median (95%CI)	Log-rank P-value	Median (95%CI)	Log-rank P-value	Median (95%CI)	Log-rank P-value
NRTIs + INSTIs	14	PR or SD [a] N=8	NR (3.5, NR)	0.0364	2.8 (1.4, NR)	0.1853	13.0 (6.3, NR)	0.1339
NRTIs + non-INSTIs	6	PR or SD [a] N=3	2.3 (1.2, 3.7)		2.3 (0.2, 6.0)		5.8 (0.2, 9.2)	

Footnote: [a] SD for at least 24 weeks; NR not reached; CI, confidence interval; cART, combination antiretroviral therapy; NRTIs, Nucleoside Reverse Transcriptase Inhibitors; INSTIs, Integrase Strand-Transfer Inhibitors; PR, Partial Response; SD, Stable Disease; NR: No Response.

eTable 3. PD-L1 expression and response.

Type of cancer	PD-L1 expression	Response (RECIST 1.1)
NSCLC	Positive	PR
NSCLC	Positive	PR
NSCLC	Positive	PR
NSCLC	Positive	SD
SCLC	Negative	PD
NSCLC	Negative	PD
Bladder cancer	Negative	PD
Melanoma	Negative	PD
NSCLC	Negative	PD
Melanoma	Negative	SD
Anal cancer	Negative	SD
NSCLC	Negative	PD
NSCLC	Negative	SD

eTable 4. Molecular classification by NGS of tumors.

ID patient	Tumor Type	Sample	Mutations						CNV	Comments
			KRAS	EGFR	BRAF	NRAS	STK11	TP53		
01100001	Bladder Cancer	Plasma	wt	wt	wt	NE	NE	NE	NE	Untested regions
00200002	NSCLC	Plasma	wt	wt	wt	**G12V**	wt	**c.560-1G>A**	**NRAS amplification**	
00200003	NSCLC	Plasma	NE	NE	NE	NE	NE	NE	**–**	Quality control parameters out of range
00200004	NSCLC	Plasma	wt	wt	wt	wt	wt	wt	**–**	
01100005	NSCLC	Plasma	**G12C**	wt	**G596R**	wt	**G268R**	**R248L**	**–**	
10100006	NSCLC	Plasma	wt	wt	wt	wt	wt	**V218G**	**–**	
05300007	NSCLC	FFPE	**G12V**	wt	wt	wt	wt	**C177F**	**–**	
03500008	NSCLC	Plasma	**G12F**	wt	wt	wt	wt	wt	**–**	
00200009	NSCLC	FFPE	**G12V**	wt	**V600E**	wt	wt	**G245C +** V151I*	**–**	*Germline mutation
01100010	Melanoma	Plasma	wt	wt	wt	wt	wt	wt	**–**	
00200011	NSCLC	FFPE	wt	wt	wt	wt	wt	**R273L**	**HER2 amplification**	
03500012	NSCLC	FFPE	**Q61H**	wt	wt	wt	**P281fs*6**	wt	**–**	
03600013	NSCLC	FFPE	wt	wt	wt	wt	**E165***	**K132+**	**–**	
04600015	Anal Cancer	Plasma	wt	wt	wt	NE	NE	NE	NE	Untested regions
05300016	SCLC	FFPE	wt	wt	wt	wt	wt	wt	**–**	
00200017	NSCLC	Plasma	wt	wt	wt	NE	NE	NE	NE	Untested regions
00200018	NSCLC	FFPE	**G12C**	wt	wt	wt	wt	**R248L**	**–**	
05300019	Melanoma	Plasma	wt	wt	wt	wt	wt	wt	**–**	
03500020	NSCLC	Plasma	wt	wt	wt	wt	wt	wt	**–**	

Footnote: FFPE, formalin-fixed paraffin-embedded; wt, wild type; NE, non-evaluable; CNV, copy number variations

eTable 5. Pre-treatment most differentially expressed genes between patients with- and without clinical benefit to durvalumab.

Gene	FC No CB vs. CB	SE	Lower Confidence Limit	Upper Confidence Limit	P-value	Adjusted P-value	Annotation	Probe ID
TREM1-mRNA	-5.88	1.28	-8.39	-3.37	0.000778	0.764	Myeloid Compartment	NM_001242589.2:101
CCL3/L1-mRNA	-5.32	1.19	-7.65	-3.00	0.000924	0.764	Cytokine and Chemokine Signaling	NM_021006.5:411
IL1B-mRNA	-6.52	1.47	-9.39	-3.64	0.000988	0.764	Cytokine and Chemokine Signaling, MAPK, Myeloid Compartment	NM_000576.2:1122
HK2-mRNA	-3.81	0.90	-5.57	-2.04	0.00118	0.764	Hypoxia, Metabolic Stress	NM_000189.4:2883
CCL4-mRNA	-4.19	1.01	-6.17	-2.21	0.00137	0.764	Antigen Presentation, Cytokine and Chemokine Signaling, Myeloid Compartment	NM_002984.2:35
LY96-mRNA	-2.59	0.62	-3.8	-1.39	0.00146	0.764	Apoptosis, Myeloid Compartment	NM_001195797.1:135
FCGR2B-mRNA	-4.65	1.16	-6.92	-2.38	0.00202	0.829		NM_001002273.1:870
CXCL3-mRNA	-3.77	0.94	-5.62	-1.92	0.00211	0.829	Cytokine and Chemokine Signaling, Myeloid Compartment	NM_002090.2:467
CXCR4-mRNA	-3.71	1.00	-5.68	-1.75	0.00303	0.982	Cytokine and Chemokine Signaling, Immune Cell Adhesion and Migration	NM_001008540.1:1060
AQP9-mRNA	-4.19	1.11	-6.38	-2.01	0.00313	0.982	Metabolic Stress	NM_001320635.1:753
EGR1-mRNA	-3.54	1.01	-5.52	-1.56	0.00436	1	Costimulatory Signaling, Interferon Signaling, Lymphoid Compartment	NM_001964.2:2034
SLC11A1-mRNA	-3.54	1.01	-5.52	-1.56	0.00494	1	Myeloid Compartment	NM_000578.3:1679
CXCL5-mRNA	-3.89	1.11	-6.08	-1.71	0.005	1	Cytokine and Chemokine Signaling, Myeloid Compartment	NM_002994.4:475
ICAM1-mRNA	-3.28	0.97	-5.18	-1.38	0.0055	1	Immune Cell Adhesion and Migration, Interferon Signaling, Matrix Remodeling and Metastasis	NM_000201.2:2253
MRC1-mRNA	-3.58	1.06	-5.65	-1.51	0.00606	1	Antigen Presentation, Myeloid Compartment	NM_002438.2:525
TNFAIP3-mRNA	-3.8	1.13	-6.02	-1.58	0.00647	1		NM_001270508.1:3240
LYZ-mRNA	-3.17	0.98	-5.09	-1.25	0.00708	1	Myeloid Compartment	NM_000239.2:381
HCK-mRNA	-2.95	0.90	-4.72	-1.18	0.00751	1	Cytokine and Chemokine Signaling, Myeloid Compartment	NM_001172129.1:325
CD36-mRNA	2.93	0.90	1.17	4.70	0.00771	1	Antigen Presentation, Matrix Remodeling and Metastasis	NM_001001548.2:705
ITGAX-mRNA	-3.28	1.04	-5.33	-1.24	0.00846	1	Immune Cell Adhesion and Migration, Matrix Remodeling and Metastasis, Myeloid Compartment	NM_000887.4:561
IL1RN-mRNA	-3.07	0.97	-4.97	-1.17	0.00903	1	Cytokine and Chemokine Signaling, Myeloid Compartment	NM_000577.3:480
IL7R-mRNA	-2.55	0.84	-4.21	-0.90	0.0116	1	Cytokine and Chemokine Signaling, JAK-STAT Signaling, PI3K-Akt	NM_002185.3:1355

VEGFA-mRNA	-2.18	0.74	-3.63	-0.73	0.0122	1	Angiogenesis, Hypoxia, MAPK, Metabolic Stress, PI3K-Akt	NM_001171623.1:2212
CCL2-mRNA	-2.9	0.99	-4.84	-0.97	0.0124	1	Cytokine and Chemokine Signaling, Myeloid Compartment	NM_002982.3:303
SOCS1-mRNA	-1.97	0.66	-3.27	-0.67	0.0126	1	Antigen Presentation, Interferon Signaling, JAK-STAT Signaling	NM_003745.1:1022
CDKN2B-mRNA	2.28	0.79	0.73	3.83	0.0136	1	Cell Proliferation, Metabolic Stress, TGF-beta Signaling	NM_004936.3:906
JAG1-mRNA	2.32	0.81	0.74	3.9	0.0138	1	Angiogenesis, Notch Signaling	NM_000214.2:3509
IRF7-mRNA	-2.35	0.84	-3.99	-0.71	0.0159	1	Interferon Signaling	NM_004029.2:1705
CCL14-mRNA	2.50	0.88	0.77	4.23	0.0161	1	Cytokine and Chemokine Signaling	NM_032962.4:253
CD48-mRNA	-2.71	0.96	-4.59	-0.84	0.0161	1	Costimulatory Signaling, Lymphoid Compartment	NM_001778.3:413
MARCO-mRNA	-1.26	0.45	-2.15	-0.38	0.0176	1	Myeloid Compartment	NM_006770.3:1435
TNFRSF1B-mRNA	-2.39	0.87	-4.1	-0.68	0.018	1	NF-kappaB Signaling	NM_001066.2:596
ITPK1-mRNA	1.74	0.64	0.49	3.00	0.0186	1	Angiogenesis	NM_001142593.2:958
CD68-mRNA	-2.50	0.96	-4.39	-0.62	0.0232	1		NM_001251.2:1140
CD45RO-mRNA	-2.33	0.93	-4.15	-0.51	0.0275	1		NM_080921.3:258
ITGB2-mRNA	-2.45	0.98	-4.37	-0.53	0.0281	1	Immune Cell Adhesion and Migration, Matrix Remodeling and Metastasis	NM_000211.3:1412
P4HA1-mRNA	-2.20	0.91	-3.98	-0.41	0.0327	1		NM_000917.3:805
TPM1-mRNA	1.71	0.71	0.31	3.11	0.0336	1	Angiogenesis	NM_000366.5:830
CX3CL1-mRNA	-1.80	0.75	-3.27	-0.33	0.0337	1	Cytokine and Chemokine Signaling, Lymphoid Compartment	NM_002996.3:1850
CSF1-mRNA	-1.88	0.78	-3.42	-0.35	0.0347	1	Cytokine and Chemokine Signaling, MAPK, Myeloid Compartment, PI3K-Akt	NM_000757.5:251
MXI1-mRNA	-2.17	0.91	-3.95	-0.38	0.035	1		NM_001008541.1:2037
IFIT2-mRNA	-3.72	1.55	-6.75	-0.68	0.0351	1	Cytotoxicity, Interferon Signaling	NM_001547.4:1995
ATF3-mRNA	-2.57	1.08	-4.70	-0.45	0.0353	1	Antigen Presentation	NM_001674.3:1487
LILRB2-mRNA	-1.85	0.77	-3.37	-0.33	0.0358	1	Costimulatory Signaling, Myeloid Compartment	NM_001278405.1:256
FCGR2A-mRNA	-2.11	0.89	-3.86	-0.36	0.0361	1		NM_021642.3:60
PFKFB3-mRNA	-2.01	0.85	-3.67	-0.34	0.0364	1	Hypoxia, Metabolic Stress	NM_004566.3:1925
VEGFC-mRNA	1.91	0.82	0.30	3.52	0.04	1	Angiogenesis, MAPK, PI3K-Akt	NM_005429.4:588
COL11A1-mRNA	1.77	0.77	0.27	3.27	0.0411	1	Matrix Remodeling and Metastasis, Myeloid Compartment	NM_001854.3:5744
TNFSF13-mRNA	-1.87	0.82	-3.48	-0.27	0.0432	1	NF-kappaB Signaling	NM_003808.3:810

Footnote: FC, Fold change; CB: Clinical Benefit; SE, Standard Error

eTable 6. Correlation of basal CD4+, CD8+ T cell counts and antitumoral efficacy.

Baseline CD4 CD8 ratio CD4/CD8 and Clinical Benefit				
		Yes (N=8)	No (N=8)	P Value Test
CD4+T(cells/mm^3)				
	n	8	8	
	Mean (SD)	484.00 (228.78)	390.13 (153.79)	T-Test: 0.3518
	Median [Q1,Q3]	456.50 [357.50, 567.50]	312.00 [294.00, 503.00]	
	Min, Max	164.00, 945.00	246.00, 657.00	
CD8+T(cells/mm^3)				
	n	7	8	
	Missing	1	0	
	Mean (SD)	1217.71 (1452.01)	727.50 (453.57)	Wilcoxon: 0.5347
	Median [Q1,Q3]	692.00 [596.00, 1108.00]	586.00 [351.50, 1061.50]	
	Min, Max	243.00, 4460.00	288.00, 1534.00	
CD4/CD8 ratio				
	n	7	8	
	Missing	1	0	
	Mean (SD)	0.65 (0.37)	0.74 (0.48)	T-Test: 0.7154
	Median [Q1,Q3]	0.71 [0.35, 0.78]	0.67 [0.34, 1.05]	
	Min, Max	0.07, 1.27	0.20, 1.59	

Footnote: Clinical Benefit is defined as patients with partial response (PR), complete response (CR) or long stable disease (SD) (≥ 24 weeks)

eREFERENCES

1. Schaller TH, Batich KA, Suryadevara CM, Desai R, Sampson JH. Chemokines as adjuvants for immunotherapy: implications for immune activation with CCL3. Expert review of clinical immunology 2017;13:1049-60.

2. Castellino F, Huang AY, Altan-Bonnet G, Stoll S, Scheinecker C, Germain RN. Chemokines enhance immunity by guiding naive CD8+ T cells to sites of CD4+ T cell-dendritic cell interaction. Nature 2006;440:890-5.

3. Rosell R. Mediating resistance in oncogene-driven cancers. N Engl J Med 2013;368:1551-2.

4. Mariathasan S, Turley SJ, Nickles D, et al. TGFbeta attenuates tumour response to PD-L1 blockade by contributing to exclusion of T cells. Nature 2018;554:544-8.

5. Tauriello DVF, Palomo-Ponce S, Stork D, et al. TGFbeta drives immune evasion in genetically reconstituted colon cancer metastasis. Nature 2018;554:538-43.

6. Garcia-Rendueles AR, Rodrigues JS, Garcia-Rendueles ME, et al. Rewiring of the apoptotic TGF-beta-SMAD/NFkappaB pathway through an oncogenic function of p27 in human papillary thyroid cancer. Oncogene 2017;36:652-66.

SUPPLEMENTARY FIGURES

eFigure 1. Flowchart of HIV-1-infected cancer patients enrolled in the DURVAST study.

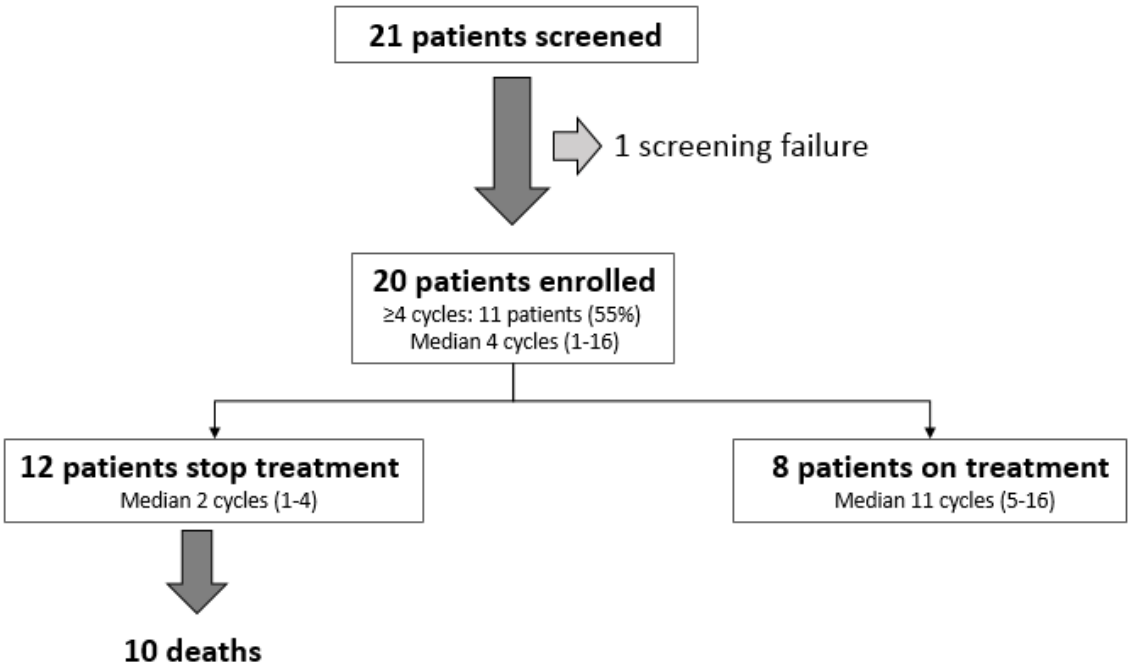

eFigure 2. Tumor response. Patients that displayed PR to treatment were all NSCLC cases. SD was achieved in three patients with NSCLC, one melanoma and one anal carcinoma.

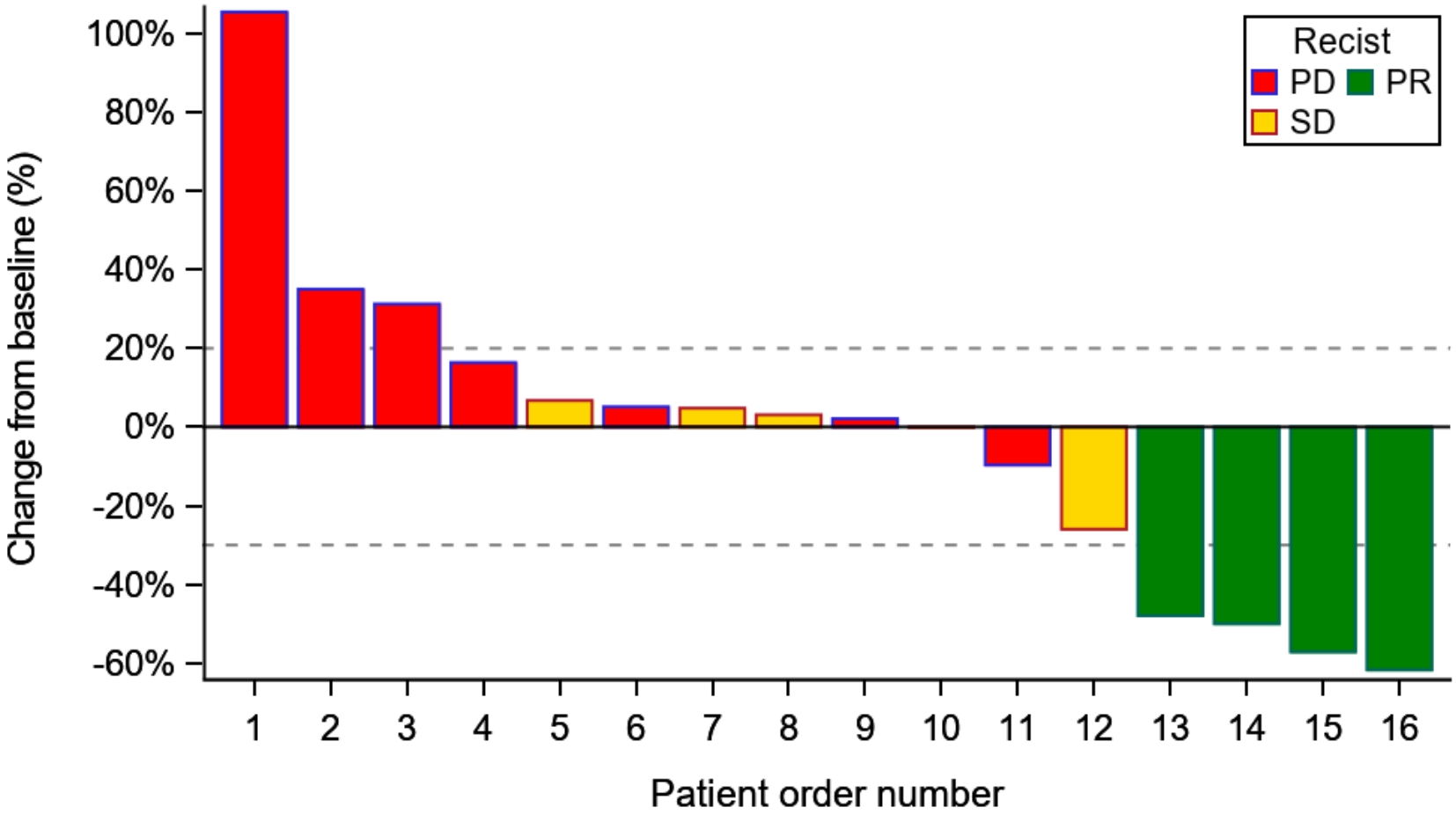

eFigure 3. A. Progression free survival of HIV-1-infected cancer patients treated with durvalumab in the DURVAST study. B. Overall survival of HIV-1-infected cancer patients treated with durvalumab in the DURVAST study.

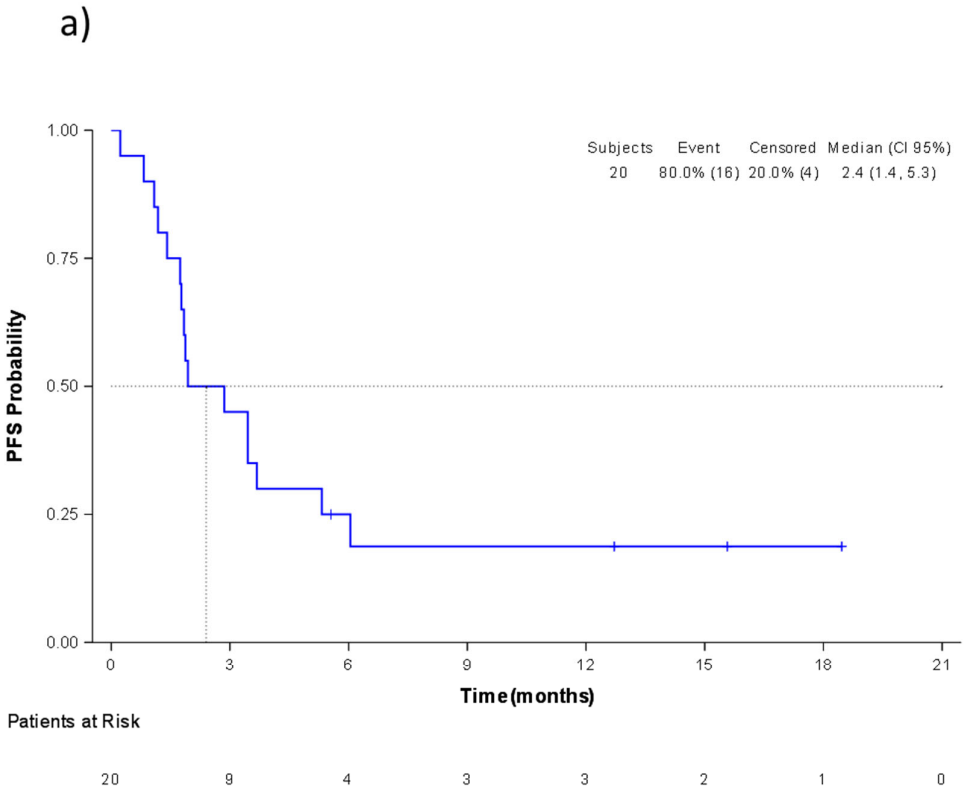

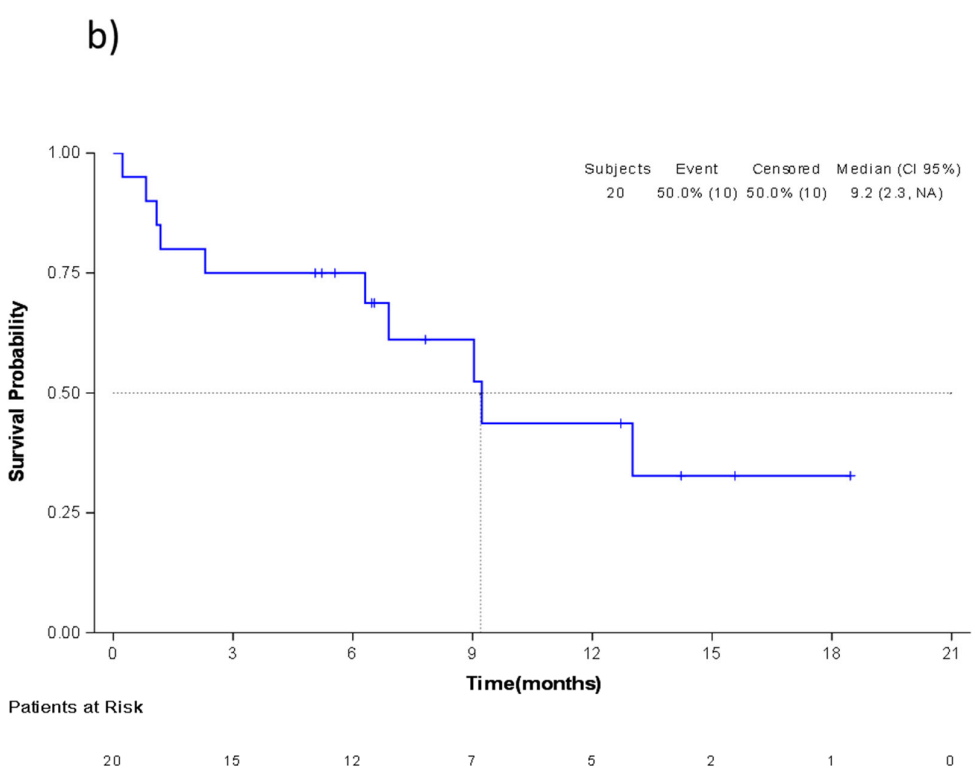

eFigure 4. A. Progression free survival of HIV-1-infected cancer patients treated with durvalumab in the DURVAST study, by PD-L1 status. B. Overall survival of HIV-1-infected cancer patients treated with durvalumab in the DURVAST study, by PD-L1 status.

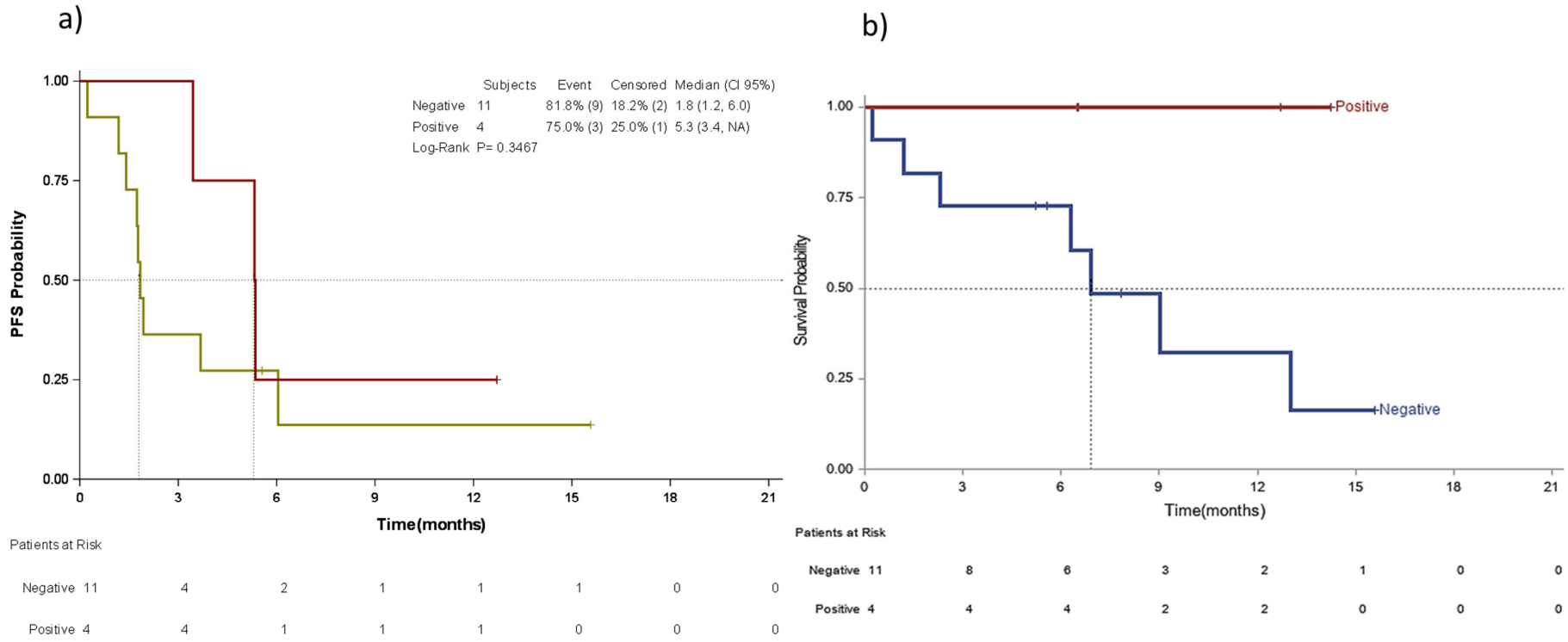

eFigure 5. Volcano plot with differentially expressed genes in patients without- versus with clinical benefit. Gene expression analysis of pre-treatment FFPE tumor tissue samples (n=14) from HIV-1-infected cancer patients included in the DURVAST study was performed using the IO 360 panel on the Nanostring platform, including patients with clinical benefit (n=7) and patients without clinical benefit (n=7). The volcano plot illustrates the log2 fold change (FC) in gene expression (no clinical benefit versus clinical benefit), and the unadjusted P-values for each gene, calculated by the nSolver software. Differentially expressed genes (P < 0.05 and Log2FC > 2 or < -2) are depicted in red, genes that had a non-significant p-value but a Log2FC > 2 or < -2 are depicted in green, blue color depicts genes that have a significant p-value but a Log2FC < 2 or > -2 and genes depicted in grey had no significant p-value nor a Log2FC < 2 or > -2. The long-dash line indicates a p-value of 0.05, and the two-dash line indicates a p-value of 0.01. All genes with a p-value < 0.05 can be found in Supplementary eTable 2. Panel-incorporated biological signature scores were calculated based on average gene expression in each signature and provided us with the two most differentially expressed signatures between patients with- and without clinical benefit: TGF beta and cytokine and chemokine signaling.

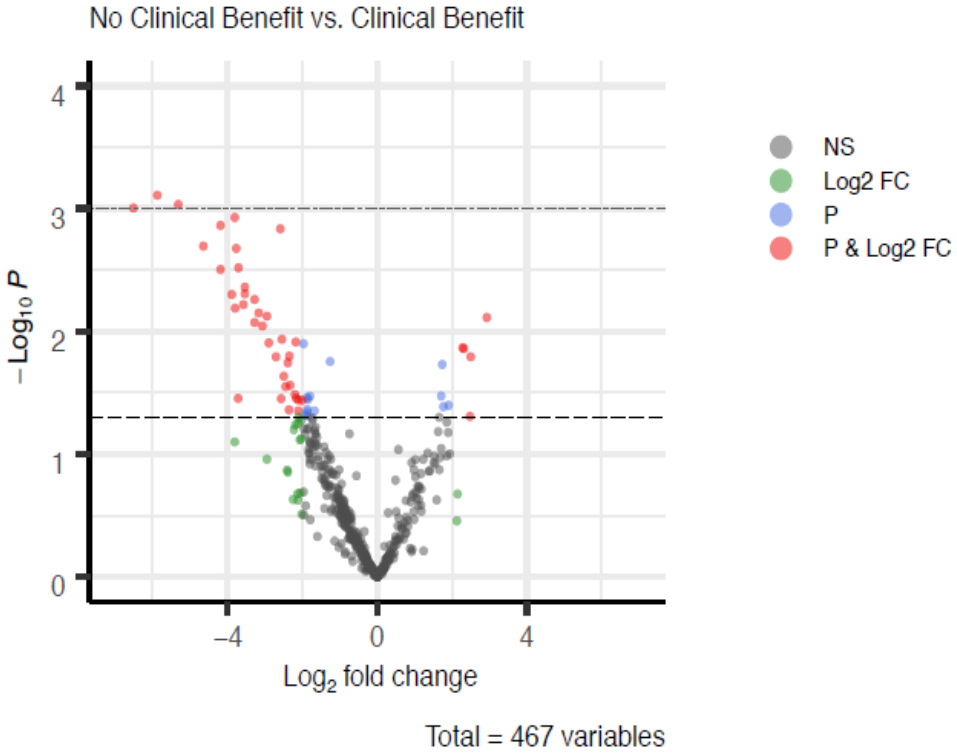

eFigure 6. Signature scores in patients with and without clinical benefit. Activation of cytokine and chemokine signaling nodes are important for immune cell recruitment to the tumor and consequent activation of a T cell response. In addition, upregulation of the TGF beta signature can induce immune evasion by enabling T cell exclusion in the tumor. Importantly, co-targeting the TGF beta pathway and PD-L1 may overcome this exclusion and can increase therapy effectiveness. Signature scores for cytokine and chemokine signaling and TGF beta signaling were calculated based on average expression of genes involved in these pathways for each patient (n=14). Patients were grouped based on clinical benefit and no clinical benefit and average scores were compared. **A.** Although not significant, cytokine and chemokine signature score tended to be lower in patients without clinical benefit (Mann-Whitney U, P = 0.097). **B.** A non-significant but tendency towards higher TGF beta signature score was found in patients without clinical benefit (Mann-Whitney U, P = 0.318). **C.** An aggregated significantly different signature score was derived from both cytokine and chemokine signaling and TGF beta signaling scores (Mann-Whitney U, P = 0.017).

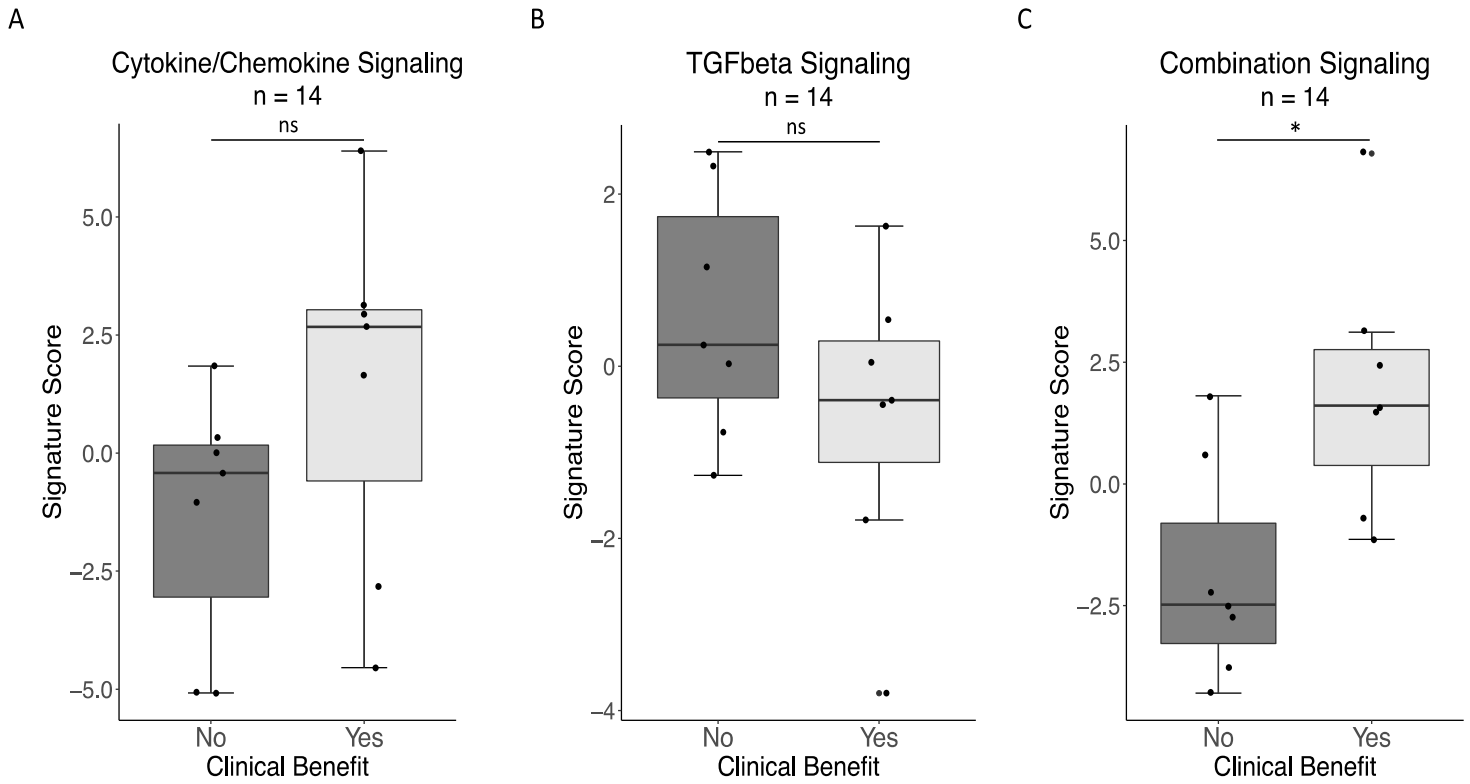

eFigure 7. Restoring CD8 T cells and latency reversal "Shock and kill strategy."